9, 2224 (1970); M. Ruegg, A. Ludi, and K. Rieder, *ibid.*, **10**, 1773 (1971).
(14) D. Nichols, "Comprehensive Inorganic Chemistry", Vol. 3, J. C. Ballar, Jr., Ed. 1st ed, Pergamon Press Ltd., Oxford, 1973.
(15) K. N. Rao, C. J. Humphreys, and D. H. Rank, "Wavelength Standards in Infrared", Academic Press, New York, N.Y., 1966.
(16) International Union of Pure and Applied Chemistry, "Tables for the Calibration of Infrared Spectrometers", Butterworths, London, 1961.
(17) W. P. Griffith and G. T. Turner, *J. Chem. Soc. A*, 858 (1970).
(18) As can be seen by the symmetry force constants for M–C stretch, $F^{A_{1g}}{}_{MC} = f_{MC} + 4f^{cis}{}_{MC,MC} + f^{trans}{}_{MC,MC}$ while $F^{E_g}{}_{MC} = f_{MC} - 2f^{cis}{}_{MC,MC} + f^{trans}{}_{MC,MC}$; the E_g mode will be higher in frequency than the A_{1g} mode if $f^{cis}{}_{MC,MC}$ is negative. This suggests that M–C bands cis to M–C will shorten slightly in order to minimize potential energy as M'–C$_1$ is stretched. Any definitive statement concerning changes in valence potential constants must wait for a detailed normal-mode calculation for the $Fe(CN)_6^{4-}$ ion.
(19) E. B. Wilson, J. C. Decius, and P. C. Cross, "Molecular Vibrations", McGraw-Hill, New York, N.Y., 1955.
(20) J. H. Schachtschneider, "Vibrational Analysis of Polyatomic Molecules, III", Technical Report No. 263-62, Shell Development Co., Emeryville, Calif.

Contribution from the Chemistry Department, University of Texas, Austin, Texas 78712

Aspects of the Structure and Bonding in Prussian Blues. A Single-Crystal Raman Study of $Mn_3[Co(CN)_6]_2 \cdot xH_2O$ and $Cd_3[Co(CN)_6]_2 \cdot xH_2O$

BASIL I. SWANSON

Received May 13, 1975

AIC50336B

Single-crystal polarized Raman spectra have been obtained for the Prussian Blue analogs $Mn_3[Co(CN)_6]_2 \cdot xH_2O$ and $Cd_3[Co(CN)_6]_2 \cdot xH_2O$ and their Raman-active fundamentals have been assigned. Raman spectra have also been obtained for both salts following dehydration and after substitution of ammonia for water. Large shifts are observed for the $Co(CN)_6^{3-}$ modes in going from aqueous solution to the Prussian Blue lattices; the Co–C stretching modes increase by 65–75 cm^{-1}. The observed shifts for the Co–C and C–N stretching modes can be reproduced by inclusion of M–N (M = Mn or Cd) interactions without changing the intramolecular potentials except for an increase in the valence C–N stretching constant. The high value estimated for the Mn–N force constant and the calculated change in f_{CN} provide evidence for an unusually strong Mn–N interaction and for a $d\pi$–$p\pi^*$ overlap between the manganese and the nitrogen end of the cyanide. Results obtained for the dehydrated samples show that the M–N bond strength increases as water is removed. Also, both salts undergo a phase change to a low-symmetry space group as water is removed. Raman data show that substitution of ammonia for water in the cadmium salts destroys the strong Prussian Blue lattice generating a double salt of the type $[Cd(NH_3)_n][Co(CN)_6]_2 \cdot yNH_3$.

Introduction

There has been considerable interest over the years in the series of transition metal cyanides, referred to as Prussian Blues. These salts are highly insoluble, indicating the presence of unusually strong interionic forces. More importantly, these cyano complexes, notably cupric ferrocyanide, act as semipermeable membranes.

While a great deal of work has been done on these simple cyanides, their structures have remained a mystery until very recently. Early structural work was based on powder samples as single crystals could not be obtained. Ludi's recent success in obtaining single crystals of manganous cobalticyanide,[1] $Mn_3[Co(CN)_6]_2 \cdot xH_2O$, and other Prussian Blue analogues[2] has provided a consistent structural model for these cyano complexes. Ludi's structural work, and the availability of single crystals, now make it possible to carry out detailed vibrational spectroscopic studies which were not possible with powder samples.

The molecular vibrations of Prussian Blues are interesting from two standpoints. First, the structural simplicity of the Prussian Blues makes them ideal model systems for studying molecular transport through membranes. Similar studies on noncrystalline membranes are difficult since the local guest molecule environment is either unknown or variable. With a crystalline membrane it should be possible to probe directly the interactions between the membrane lattice and the guest molecule using vibrational spectroscopy. Perturbations of the host membrane molecular vibrations as water is removed and replaced by other small molecules provide direct information concerning the membrane bonding as a function of the guest molecule. Similarly, shifts in the guest molecule's molecular vibrations in going from an isolated envionment to the membrane lattice will tell us something of the bonding changes in the guest molecule.

Prussian Blues are intriguing model systems for studying membranes for several reasons. There are only three discrete types of sites for the guest molecule, and each has high symmetry.[1,2] Thus, the guest–host interactions are few and relatively simple. The high space group symmetry of the Prussian Blues, $Fm3m$, and the high site symmetry of the hexacyanide moieties, O_h, simplifies both vibrational assignments and the interionic interactions. Also, the abundance of information on related cyano complexes provides adequate basis for comparative studies. The principal ingredient of the Prussian Blues, the transition metal hexacyanide, has been probed by vibrational spectroscopy,[3,4] electronic spectra,[5] and MO calculations.[5,6] The cubic $Cs_2LiM(CN)_6$ salts, which are structurally similar to the Prussian Blues, have been studied in detail using vibrational spectroscopy[7,8] and x-ray crystallography.[9,10] The effort spent on the dicesium lithium salts and the recent emergence of related cyanides[11,12] should simplify our present effort.

The bonding in Prussian Blues is also interesting from the standpoint of their unusually strong interionic potentials. In ionic species, external forces often perturb the internal modes of vibration in a dramatic way. The frequency shifts observed for $M(CN)_6^{3-}$ internal modes in going from aqueous solution to the $Cs_2LiM(CN)_6$ lattices are substantial.[7,8] Surprisingly, even the high-frequency C–N stretching modes were observed to shift. Normal-mode calculations for $Cs_2LiCo(CN)_6$ and $Cs_2LiFe(CN)_6$,[7] where interionic potentials were included, have shown that these large frequency shifts could be reproduced without changing the intramolecular potential function; except for a slight increase in the valence C–N force constant.

For the dicesium lithium salts the large frequency shifts result primarily from the strong Li–N interaction.[4b,7] Since the structures of the $Cs_2LiM(CN)_6$ salts closely parallel those of Prussian Blues and since in place of a Li–N interaction there is now a much stronger M–N interaction (where M is a di-

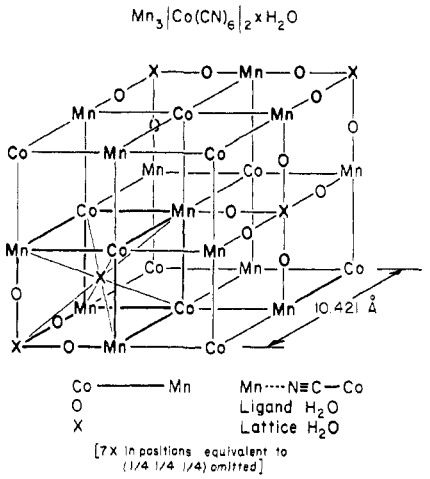

Figure 1. Schematic of the $Mn_3[Co(CN)_6]_2 \cdot xH_2O$ lattice.

or trivalent transition metal), even larger perturbations are expected for the $M(CN)_6^{n-}$ internal modes.

This report is concerned with single-crystal Raman spectra of $Mn_3[Co(CN)_6]_2 \cdot xL$ and $Cd_3[Co(CN)_6]_2 \cdot xL$ (where L = H_2O, D_2O, NH_3, ND_3) and the corresponding dehydrated samples. The single crystals used in this study were kindly supplied by Gary Beall and W. O. Milligan.[13]

Experimental Section

Both $Mn_3[Co(CN)_6]_2 \cdot xH_2O$ and $Cd_3[Co(CN)_6]_2 \cdot xH_2O$ crystallize in the space group $Fm3m$ with the $Co(CN)_6^{3-}$ moieties statistically disordered in the octahedral site at the origin of the unit cell.[1,2] The counter transition metals occupy the other octahedral sites along the cell edges [the 4b position (0, 0, 1/2) etc.]. Water molecules are present in the tetrahedral holes and are also found coordinated to the counter transition metal (Mn^{2+} or Cd^{2+}) when the $Co(CN)_6^{3-}$ moiety is not present. Recent crystallographic studies also indicate that water may be present in the 4a positions when the $Co(CN)_6^{3-}$ ion is missing.[14] Thus, in addition to the coordinated water, there are two different types of zeolitic water present in the Prussian Blue lattice. A schematic of the structure is shown in Figure 1.

The molecular vibrations for the Prussian Blues are most conveniently discussed by considering the guest molecule and the $M^{II}_3[Co(CN)_6]_2$ framework separately. It is not possible to assign the guest molecules vibrations in detail since the water structure is not known. Thus, those modes which can be attributed to guest molecules will simply be compared with the free-molecule vibrations.

The selection rules for the $M^{II}_3[Co(CN)_6]_2$ framework are somewhat complicated by the presence of coordinated water: in a strict sense the local symmetry of the M^{II} ion is not octahedral. However, the observed spectra do not deviate markedly from that expected using $Fm3m$ selection rules. Thus, selection rules based on an O_h factor group will be used here.

As we are interested in comparing the molecular vibrations of the Prussian Blues with those of $Cs_2LiCo(CN)_6$ and since the structures are essentially the same,[15] the Raman-active modes will be labeled as were those of the dicesium lithium salts. For both salts A_{1g} and E_g symmetry C–N and Co–C stretching modes and F_{2g} symmetry Co–C–N and C–Co–C deformation modes are allowed in the Raman effect. There are no Raman-active lattice modes for the $M^{II}_3[Co(CN)_6]_2$ framework.

The symmetry species of the observed Raman modes can be distinguished using two different crystal orientations as has been described earlier.[8] Four scans were used. In scan (001)[(100)(100)^s](010) A_{1g} and E_g modes are allowed, while for (001)[(100)(001)^s](010) only F_{2g} modes are allowed. A_{1g} and E_g modes can be distinguished using scans (10$\bar{1}$)[(101)(101)^s](010) and (10$\bar{1}$)[(101)(10$\bar{1}$)^s](010) (where A_{1g}, E_g, and F_{2g} modes and only E_g modes are allowed, respectively). The notation used here is that proposed by Swanson.[16] The crystals used in this study were small (typically, cubes less than 0.4 mm on an edge). Consequently, polarization data were obtained using an oil immersion cell designed for small crystals.[17]

Raman spectra for dehydrated single crystals and for crystals where ammonia was substituted for water were observed using the evacuable cell shown in Figure 2. The crystal was coupled to an optical flat using silicone grease. The crystal could then be dehydrated by heating the oil reservoir to ca. 70°C while the cell was evacuated. Dehydration was complete in 24 hr as evidenced by the Raman spectrum;[18] longer periods of dehydration resulted in no change in the Raman spectrum. Ammonia could then be substituted by exposing the dehydrated crystal to ca. 100 mm of NH_3. Using the cell shown in Figure 2 the Raman spectra for a particular crystal could be obtained before and after dehydration and after exposure to NH_3.

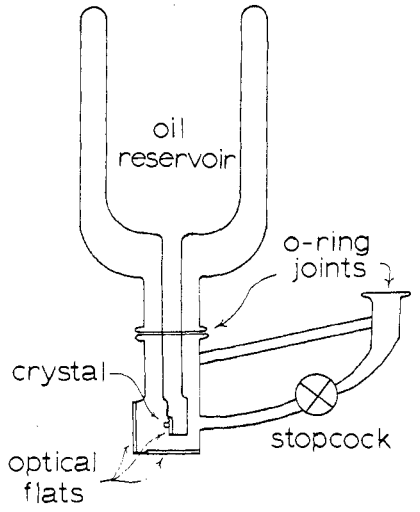

Figure 2. Evacuable single-crystal Raman cell.

Raman spectra were observed using a Cary 82 spectrometer and a Spectra Physics 164 Kr^+ ion laser (6472-Å line). In order to avoid damage to the crystal, the laser power was maintained at ca 100 mW at the sample. Laser damage was particularly troublesome for dehydrated crystals as they were opaque. The spectrometer was calibrated in the usual way.[4]

Assignments

$M^{II}_3[Co(CN)_6]_2$ Modes. Vibrational assignments for the $Co(CN)_6^{3-}$ internal modes can easily be made using polarization data. The four scans (001)[(100)(100)^s](010), (001)[(100)(001)^s](010), (10$\bar{1}$)[(101)(101)^s](010), and (10$\bar{1}$)[(101)(10$\bar{1}$)^s](010) for $Mn_3[Co(CN)_6]_2 \cdot xH_2O$ are presented in Figure 3. The observed spectra for the cadmium salts are similar to those of the manganese complex. For both salts two bands appear at ca. 2192 and 2172 cm^{-1} which can be assigned to ν_1 and ν_3, respectively (see Figure 3). These two C–N stretches are observed roughly 30 cm^{-1} lower for $Cs_2LiCo(CN)_6$.

Unpolarized spectra in the Co–C stretch and Co–C–N deformation region, where three bands are expected, show only a broad band at ca. 480 cm^{-1} and a weak shoulder at ca. 440 cm^{-1}. Both ν_2 and ν_4 contribute to the resolved feature at ca. 480 cm^{-1}, as can be verified by comparing scans (10$\bar{1}$)[(101)(101)^s](010) and (10$\bar{1}$)[(101)(10$\bar{1}$)^s](010). Note that for scan (10$\bar{1}$)[(101)(10$\bar{1}$)^s](010), where the A_{1g} mode is not allowed and the E_g mode is stronger,[19] the apparent peak position for the 480-cm^{-1} band is lowered 10 cm^{-1}. For the cadmium complex both bands were cleanly resolved even in the unpolarized spectra. The Co–C stretching modes are observed roughly 50 cm^{-1} lower in the $Cs_2LiCo(CN)_6$ salt.

At first glance, it is tempting to assign the remaining band at ca. 440 cm^{-1} to the F_{2g} Co–C–N deformation, ν_{10}. However, for the dicesium lithium salt ν_{10} is observed at ca. 480 cm^{-1}. Inasmuch as ν_{10} does not shift in going from $Co(CN)_6^{3-}$(aq) to $Cs_2LiCo(CN)_6$[8] and since this same mode is also unshifted in going from $Fe(CN)_6^{4-}$(aq) to $Cs_2MgFe(CN)_6$,[20] it is unlikely that it should appear 40 cm^{-1} lower for the Prussian Blues. It is likely that ν_{10} is around 480 cm^{-1} for both $Mn_3[Co(CN)_6]_2 \cdot xH_2O$ and $Cd_3[Co(CN)_6]_2 \cdot xH_2O$

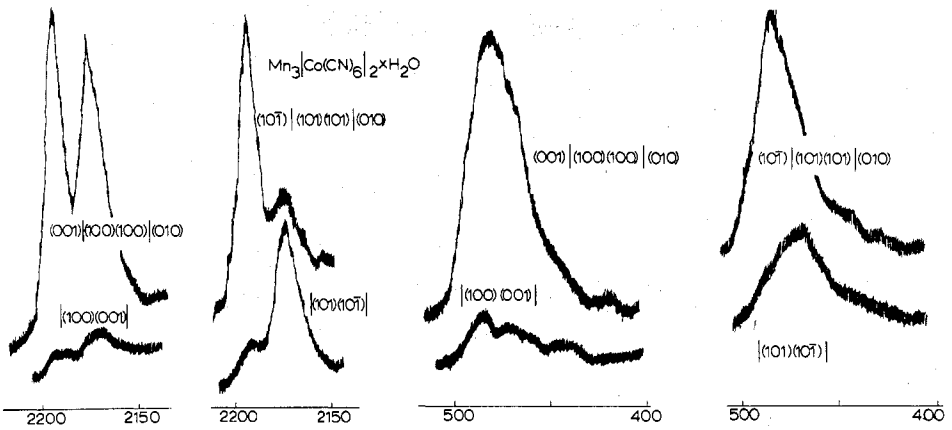

Figure 3. Polarized Raman scattering from $Mn_3[Co(CN)_6]_2 \cdot xH_2O$ (cm^{-1}).

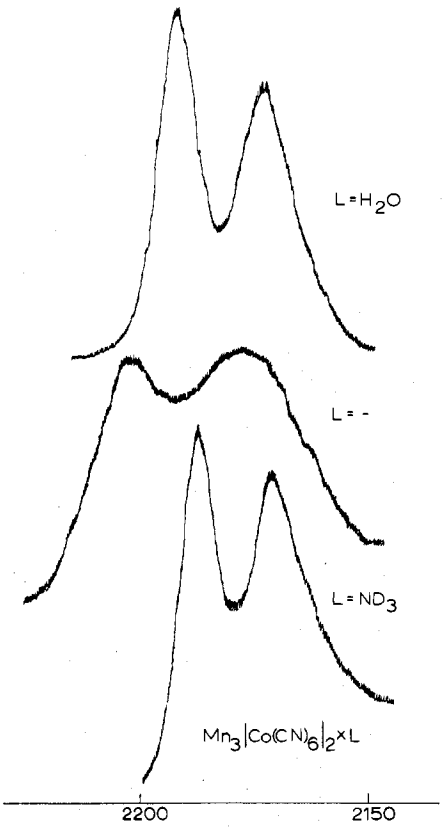

Figure 4. Raman spectra of $Mn_3[Co(CN)_6]_2 \cdot xL$ (L = H_2O, NH_3, and nothing) in the CN stretch region (cm^{-1}).

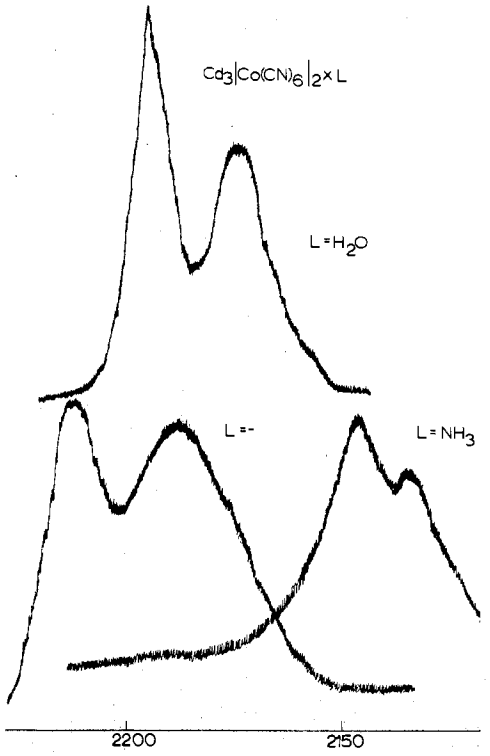

Figure 5. Raman spectra of $Cd_3[Co(CN)_6]_2 \cdot xL$ (L = H_2O, NH_3, and nothing) in the CN stretch region (cm^{-1}).

and is simply obscured by the intense A_{1g} Co–C stretch.

The origin of the 440-cm^{-1} band is not understood at this time. It is clear that the mode cannot be assigned to a ligand vibration since it is observed for the dehydrated crystals and is unshifted when NH_3 is substituted for H_2O. A clear understanding of the 440-cm^{-1} band and a definitive assignment for the F_{2g} Co–C–N deformation must await a vibrational study of ^{13}C- and ^{15}N-substituted species.

Polarized Raman spectra in the low-energy region show an F_{2g} symmetry mode at 200 cm^{-1} which can be assigned to the C–Co–C deformation ν_{11}. This band is observed in approximately the same place for the $Cs_2LiCo(CN)_6$ salt.

The observed Raman spectra for both salts change dramatically as water is removed; the C–N stretch regions for both salts are shown in Figures 4 and 5. The Co–C and C–N stretching modes shift to higher frequency and the C–Co–C deformation splits into two components. It should also be noted that the quality of the spectra decreased significantly and the bands appear to broaden as water is removed.

While the spectra for the normal and dehydrated crystals of the cadmium and manganese spectra are quite similar, they differ vastly for the NH_3-substituted species. The spectrum for $Mn_3[Co(CN)_6]_2 \cdot xNH_3$ is nearly identical with that of the hydrated sample (Figure 4). However, addition of NH_3 to the cadmium complex significantly perturbs the $Co(CN)_6^{3-}$ modes. The C–N stretching modes shift down ca. 45 cm^{-1} and the A_{1g} Co–C mode decreases by 80 cm^{-1} while the C–Co–C deformation decreases by 57 cm^{-1}. These significant shifts will be discussed below.

In addition to the modes discussed above, one additional band at ca. 340 cm^{-1} was observed for the cadmium complex. The fact that this mode does not shift when ammonia is substituted for water or when a deuterated ligand is used clearly indicates that this band involves motion of the $Cd_3[Co(CN)_6]_2$ framework. One possible explanation for this band is that it is the Co–C–N deformation of F_{1g} symmetry. This mode, which is not allowed if the crystal is strictly $Fm3m$, is active since the Co atom site symmetry is lowered by virtue of water coordination to the cadmium. While the observed position of this mode in the cadmium complex is in good

Table I. Observed Raman Modes (cm^{-1}) for the $Co(CN)_6^{3-}$ Moiety in $Mn_3[Co(CN)_6]_2 \cdot xL$ and $Cd_3[Co(CN)_6]_2 \cdot xL$ (L = H_2O, NH_3, -)[a]

	$Co(CN)_6^{3-}$ [b]	$Cs_2LiCo(CN)_6$ [c]	$Mn_3[Co(CN)_6]_2 \cdot xL$			$Cd_3[Co(CN)_6]_2 \cdot xL$		
			L = H_2O	L = -[d]	L = NH_3	L = H_2O	L = -[d]	L = NH_3
$\nu_1(A_{1g}, CN)$[a]	2153.3	2161.6	2190.8	2201	2186.6	2193.8	2212.5	2146.5
$\nu_2(A_{1g}, CoC)$	410.5	431.1	485	503	475	484		403
$\nu_3(E_g, CN)$	2137.0	2150.8	2171.8	2175	2170	2173.8	2188.0	2135.5
$\nu_4(E_g, CoC)$	(398)	418.1	470	488	463	459	~480	
$\nu_{10}(F_{2g}, CoCN)$	482	484.6	~480[e]	~480[e]	~480[e]	~480[e]	~480[e]	485
			445	442	440	439	433	
$\nu_{11}(F_{2g}, CCoC)$	115	189.9	202	213, 183.5	197	185	194, 169	128

[a] The fundamental modes for the $Mn_3[Co(CN)_6]_2 \cdot xL$ and $Cd_3[Co(CN)_6]_2 \cdot xL$ have been labeled the same as those of $Cs_2LiCo(CN)_6$ (see ref 7). [b] Reference 4a. [c] Reference 8. [d] L = - denotes the Prussian Blue complexes with water removed. [e] Assumed value.

Table II. Observed Raman Modes (cm^{-1}) for Ammonia in $Cd_3[Co(CN)_6]_2 \cdot xNH_3$ and $Mn_3[Co(CN)_6]_2 \cdot xNH_3$

Description	NH_3	$Cd_3[Co(CN)_6]_2 \cdot xL$		$Mn_3[Co(CN)_6]_2 \cdot xL$		$[Cd(NH_3)_6]Cl_2$	$[Mn(NH_3)_6]Cl_2$
		L = NH_3	L = ND_3	L = NH_3	L = ND_3		
$\nu_a(NH_3)$	3414	3365 m, br	2509 m, br	3380 w, br	2399	3335[a]	
$\nu_s(NH_3)$	3336	3282 s	2387 s	3298 s	2387	3250[a]	
$\nu(NH_3)$		3177 br, w		3175 vw, br	2353		
		3131 w	2327 w	3132 w	2322		
		3113 w		3115 w			
$\delta_d(NH_3)$	1628	1603 w	1174 w	1606 w		1585[22]	1592[22]
$\delta_s(NH_3)$	950	1302 w	918 w	~1306 vw, br		1101[22]	1134[22]
?		709 vw	709 vw				
$\rho_r(NH_3)$		560 w, br	552 w, br	571 w		613[22]	617[22]
$\nu(MN)$		345 m	304 m	342 w		298[22]	307[22]

[a] J. M. Terrasse, H. Poulet, and J. P. Mathieu, *Spectrochim. Acta*, **20**, 305 (1964).

agreement with that expected for ν_5,[7,8] it is somewhat perplexing that this mode does not shift for the ammoniated species as did the other $Co(CN)_6^{3-}$ internal modes. It is possible that ν_5 is simply insensitive to the local $Co(CN)_6^{3-}$ environment.

The above discussed $Co(CN)_6^{3-}$ modes did not shift upon isotopic substitution of the ligand (H_2O, D_2O; NH_3, ND_3) further substantiating the above assignments. The observed $Co(CN)_6^{3-}$ modes for the normal, dehydrated, and ammonia-substituted samples of the manganese and cadmium complexes are compared with those of $Co(CN)_6^{3-}$(aq) and $Cs_2LiCo(CN)_6$ in Table I.

Ligand Modes. In general, the ligand modes were quite weak and, in many instances, unobserved. This is not surprising in view of the poor scattering power of the small guest molecules and the small crystal size. For the ammoniated species the N–H stretch regions were quite complex, while for the other NH_3 fundamental modes only single bands were observed. It is likely that the N–H stretching modes for both zeolitic and coordinated ammonia are observed while for the weaker fundamental only the coordinated ammonias are observed. Most of the observed bands agree with those expected for coordinated NH_3 rather than zeolitic NH_3. The observed NH_3 bands are compared with $[Cd(NH_3)_6]Cl_2$[21] in Table II.

The situation for the hydrated samples is worse as most of the bands are unobserved. For the D_2O-substituted cadmium complex, the D–O stretch region exhibited bands at 2630 and 2610 cm^{-1}. All that can be said is that these observed modes agree with what would be expected for coordinated water.

Discussion

The observed spectra reveal something of both the structure and bonding in Prussian Blue complexes; the structural implications will be discussed first. The general agreement with *Fm3m* selection rules for the manganese complex and the quality of the polarization data are consistent with an octahedral environment for the $Co(CN)_6^{3-}$ moiety in this complex. The observation of the F_{1g} Co–C–N deformation mode for $Cd_3[Co(CN)_6]_2 \cdot xH_2O$ indicates that the $Co(CN)_6^{3-}$ site symmetry is lower than O_h in the cadmium complex.

One possible explanation is that the Cd–OH_2 and Cd–NC interactions differ significantly while the Mn–OH_2 and Mn–NC bond strengths are similar. The $Co(CN)_6^{3-}$ moiety in the manganese complex would see an isotropic environment while that in the cadmium complex would be anisotropic. Certainly, the Cd–NC interaction would depend strongly on whether the ligand trans to the –NC group is a cyanide or water. This explanation is in agreement with recent crystallographic studies of Beall and Milligan[14] on $Cd_3[Co(CN)_6]_2 \cdot xH_2O$ which show the Cd–O bond to be significantly longer than the Cd–N bond.

The Raman spectra for both salts change dramatically as water is removed. In addition to the shifts observed for the $Co(CN)_6^{3-}$ modes (discussed below) the F_{2g} C–Co–C deformation mode splits into two components indicating that the Co site symmetry has been lowered. The modes broaden (see Figure 4) and the quality of the spectra decreases. Furthermore, as water is removed, the crystals were observed to become opaque, changing from colorless to pale green. All of the above indicate that the crystal undergoes a phase change to a lower symmetry space group as water is removed. Crystallographic studies of $Mn_3[Co(CN)_6]_2 \cdot xH_2O$ as water is removed also support this suggestion.[18] Upon dehydration, the lattice constant decreases by ca. 0.2 Å and scattering becomes extremely diffuse. Both the x-ray and Raman data point to a first-order phase change with concomitant fracturing of the crystal.

The similarity of the Raman results for the Cd and Mn complexes strongly suggest that the Cd salt undergoes a similar phase change upon dehydration. This finding is in direct contrast with Ludi's recent claim that the structure of the Cd salt does not change upon dehydration.[22] There are, however, significant differences between the method used by Ludi and that reported here for removal of water. Ludi employed an N_2 gas flow system where the gas stream was heated to 30°C. In view of the extreme hygroscopic nature of the dehydrated species, it is likely that Ludi was unable to remove completely the H_2O under the mild conditions employed and was, therefore, looking at a partially dehydrated crystal.

Finally, it is appropriate to consider the structural implications of the dramatic change in the Raman spectra of the Cd complex as NH_3 is substituted for H_2O (Figure 5 and Table I). The peak positions and general appearance of the spectrum for $Cd_3[Co(CN)_6]_2 \cdot xNH_3$ agree remarkably well with that of $Co(CN)_6^{3-}$ ion in aqueous solution (Table I).[4a] The large shifts in C–N and Co–C stretching modes alone indicate that the strong Cd–N interaction has been broken. The above, combined with the observation that the ammoniated crystal crumbles when touched and dissolves in water, suggests that a double salt $[Cd(NH_3)_n]_3[Co(CN)_6]_2 \cdot yNH_3$ has been formed. The similarity of the $Co(CN)_6^{3-}$ modes in $Cd_3[Co(CN)_6]_2 \cdot xNH_3$ with those of $Co(CN)_6^{3-}$(aq) is not surprising since the H-bonding environment in the ammoniated sample is probably not greatly different from that present in water.

The absence of any extreme spectral changes as the manganese salt is ammoniated shows that this complex does not form a double salt. In general, the peak positions observed for the ammoniated manganese salt agree with those of the hydrated species. The structure of the ammoniated manganese complex is probably similar to that of the hydrated salt.

Bonding Considerations

The shifts in the $Co(CN)_6^{3-}$ modes in going from aqueous solution to the $Mn_3[Co(CN)_6]_2 \cdot xH_2O$ and $Cd_3[Co(CN)_6]_2 \cdot xH_2O$ crystalline lattices are quite large. The C–N stretch modes increase by 35–40 cm^{-1} while the Co–C stretch modes increase 65–75 cm^{-1} (Table I). These shifts should be contrasted to the smaller shifts observed in going from $Co(CN)_6^{3-}$(aq) to $Cs_2LiCo(CN)_6$[7] and from $Fe(CN)_6^{4-}$(aq) to $Cs_2MgFe(CN)_6$.[20] The observed shifts for the F_{2g} C–Co–C deformation are nearly the same as that observed for the $Cs_2LiCo(CN)_6$ salt (Table I). The stretching modes are observed to shift to even higher frequencies as water is removed (Table I).

The observed shifts in the stretching modes can be explained in terms of the nature of the M–N interactions (where M denotes the metal in the 4b position); the arguments here are essentially the same as those used to discuss $Cs_2MgFe(CN)_6$ in the preceding article.[20] The M–N interactions result in an increase in the stretching modes by virtue of the symmetry constraint in the crystalline lattice which necessitates a compression of the M–N_i bond as C_i–N_i or Co–C_i is stretched. Thus, a stronger M–N bond will lead to higher observed frequencies for ν_1, ν_2, ν_3, and ν_4.

In addition, the M–N interaction also perturbs the observed C–N stretching modes by virtue of a change in the valence C–N force constant. For the $Cs_2LiCo(CN)_6$ salt[7] f_{CN} was estimated to increase by ca. 0.1 mdyn/Å while for the ferrocyanides [$Fe(CN)_6^{4-}$(aq) → $Cs_2MgFe(CN)_6$[20]] the increase was roughly 0.5 mdyn/Å. In both cases the increase in f_{CN} was attributed to electron withdrawal from the lowest filled antibonding CN^- σ MO.

The bonding implications of the observed shifts are more readily explained by considering the A_{1g} and E_g symmetry force constants. As there are insufficient data to allow a simultaneous refinement of all of the constants in either symmetry block, certain constraints are necessary. The same constraints which were used in the original treatments of $Cs_2LiCo(CN)_6$ and $Cs_2MgFe(CN)_6$ will be used here; these constraints are itemized in Table III.

The original treatments of the $Co(CN)_6^{3-}$(aq) ion and $Cs_2LiCo(CN)_6$ were carried out using data where the C–N stretching modes were corrected for anharmonicity. The anharmonicity corrections found for $Co(CN)_6^{3-}$(aq)[4a] were used to obtain ω_1 and ω_3 for the manganese salt. The calculations were carried out using Schachtschneider's force constant perturbation program.[23] For further details on the normal-mode treatment, see the preceding article. The final symmetry force constants and the differences between calculated and observed frequencies are presented in Table III. As can be seen from Table III, the large frequency shifts observed for $Mn_3[Co(CN)_6]_2 \cdot xH_2O$ and the dehydrated sample could be reproduced in this manner.

Table III. A_{1g} and E_g Symmetry Force Constants[b]

	$Co(CN)_6^{3-}$	$Cs_2LiCo(CN)_6$	$Mn_3[Co(CN)_6]_2 \cdot xL$	
			L = H_2O	L = –
F_{11}	17.64	17.99	19.06	19.43
F_{22}	2.64	2.89	3.56	3.84
F_{12}	0.43	0.68	1.39	1.63
F_{33}	17.22	17.57	18.56	18.80
F_{44}	2.49	2.74	3.45	3.69
F_{34}	0.29	0.54	1.25	1.49
F^{ν}_{Mn-N} ($\nu = A_{1g}, E_g$)		0.25	0.96	1.2
$\Delta f_{CN}(A_{1g})$[a]		0.1	0.46	0.59
$\Delta f_{CN}(E_g)$[a]		0.1	0.38	0.38
$\Delta\nu_1$[c]			0.3	0.2
$\Delta\nu_2$[c]			1.7	3.4
$\Delta\nu_3$[c]			0.1	0.0
$\Delta\nu_4$[c]			−3.1	−1.8

[a] Δf_{CN} (A_{1g}) and Δf_{CN} (E_g) refer to the change in the valence C–N force constants estimated from the refined A_{1g} and E_g constants F_{11} and F_{33}. [b] The intramolecular symmetry force constants for $Co(CN)_6^{3-}$(aq), which are uniquely defined from isotopic shift data,[4a] will be transferred directly for F_{22}, F_{12}, F_{44}, and F_{34}. These symmetry force constants will be augmented by the appropriate symmetry force constants for the null coordinates involving Mn–N stretch ($F^{A_{1g}}_{MnN,MnN}$ and $F^{E_g}_{MnN,MnN}$). Essentially, this corresponds to transferring in the intramolecular potentials involving Co–C stretch and Co–C, C–N interaction; the symmetry force constant for Mn–N stretch enters into the expressions for Co–C and C–N stretches linearly.[7] The constants $F^{A_{1g}}_{MnN,MnN}$ and $F^{E_g}_{MnN,MnN}$ will be set equal since the only difference between these constants is the cis interaction, $f^{cis}_{MnN,MnN'}$ which is expected to be negligible.[7] The symmetry constants involving C–N stretch, F_{11} and F_{33}, will be refined; this corresponds to allowing the valence C–N stretching constant to vary. [c] $\Delta\nu = \nu_{obsd} - \nu_{calcd}$.

It is interesting to compare the values obtained here for $F^{\nu}_{MN,MN}$ (ν = A_{1g} or E_g) with those obtained earlier for $Cs_2LiCo(CN)_6$ and $Cs_2MgFe(CN)_6$. The constants $F^{\nu}_{MN,MN}$ provide a crude estimate of the relative values of the valence M–N stretching constants for these systems. The value obtained for $Cs_2MgFe(CN)_6$, $F^{\nu}_{MgN,MgN}$ = 0.55 mdyn/Å, is roughly twice as great as that obtained for $Cs_2LiCo(CN)_6$, $F^{\nu}_{LiN,LiN}$ = 0.25 mdyn/Å. This difference is expected in view of the difference in oxidation states of the 4B metal. Surprisingly, the value obtained for $Mn_3[Co(CN)_6]_2 \cdot xH_2O$ is nearly twice as great as that obtained for $Cs_2MgFe(CN)_6$, even though M is divalent in both cases.[24] Clearly, the unusually strong M–N bond in Prussian Blues cannot be considered as a strictly ionic interaction.

One possible explanation for the unusual strength of the M–N bond in Prussian Blues is the presence of $d\pi$–$p\pi^*$ interaction between M and the N end of the cyanide moiety; viz.

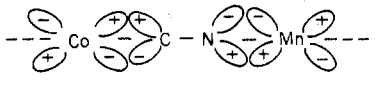

An M–N π interaction could explain the disparity in $F^{\nu}_{MN,MN}$ between Prussian Blues and $Cs_2MgFe(CN)_6$ where no such interaction is possible.

The estimated change for f_{CN} in going to the Prussian Blue lattice (Table III) lends support to such an M–N π interaction. In going from $Co(CN)_6^{3-}$(aq) to $Cs_2LiCo(CN)_6$, f_{CN} is estimated to increase ca. 0.1 mdyn/Å (see above). The corresponding change in going from $Fe(CN)_6^{4-}$ to $Cs_2MgFe(CN)_6$, ca. 0.5 mdyn/Å, is indicative of the stronger Mg–N

σ bond. If the M–N interaction is entirely a σ-type bond, we would expect f_{CN} to increase even more for $Mn_3[Co(CN)_6]_2 \cdot xH_2O$, in view of the unusual strength of the Mn–N bond. However, the estimated increase in f_{CN} for $Mn_3[Co(CN)_6]_2 \cdot xH_2O$ is slightly *less* than that calculated for $Cs_2MgFe(CN)_6$, indicating that the Mn–N bond is not strictly a σ interaction. That is, the increase in f_{CN} resulting from increased M–N σ bonding is offset by a decrease in f_{CN} resulting from Mn–N π bonding.[25]

The symmetry force constants estimated for the dehydrated salt tell us something about how the bonding in the Prussian Blue superlattice changes as water is removed. The symmetry Mn–N constant needed to reproduce the frequency shifts increases by ca. 0.24 mdyn/Å indicating a significant increase in the Mn–N bond strength. This is expected since removal of coordinated water should lead to a stronger Mn–N σ interaction if the charge density on the Mn^{2+} is to be neutralized. The above is also consistent with he observation that the lattice constant for the manganese salt decreases significantly as water is removed; the Mn–N bond length shortens with removal of coordinated water.[18] As different σ-donating molecules are introduced into the lattice, for example, NH_3, the Mn–N interaction weakens, the observed C–N and Co–C stretching frequencies decrease, and the cell size increases.

Speculation on Prussian and Turnbull's Blues

The suggestion of M–N $d\pi$–$p\pi^*$ interactions in Prussian Blues is intriguing as it implies the existence of extended overlap between metal sites via the π^* level on the CN^- moiety. It should be possible to induce electron transfer between metals by means of a charge-transfer excitation. This may provide an explanation for the conversion of ferroferricyanide, Turnbull's Blue, to ferriferrocyanide or Prussian Blue, viz.

$$-Fe^{III}-C-N-Fe^{II}- \xrightarrow{h\nu_1} [-Fe^{III}-C-N-Fe^{II}-]^* \rightarrow -Fe^{II}-C-N-Fe^{III}-$$

Thus, it is possible that ferroferricyanide is converted to ferriferrocyanide by an internal redox reaction induced by a charge-transfer excitation without the need to invoke CN^- flipping, a mechanism which seems unreasonable in view of the unusual strength of both the M'–C and M–N bonds.

The above, in conjunction with what we know of the packing forces in cubic cyanides, provides a plausible explanation for the subtle color difference between Turnbull's and Prussian Blues during the first 30 min after precipitation.[26] In the case of the $Cs_2LiM(CN)_6$ salts, the strong Li–N interaction dominates other interionic interactions and essentially determines the packing in the cubic cell.[9] It is clear from the intermolecular potentials,[4b,7] the increased stability of the dicesium lithium salts compared with the tripotassium salts,[27] and the unusually high thermal motion of the Cs atoms,[9] that the Li–N interaction dominates packing. Furthermore, the Li–N interaction is maximized when the M–C–N–Li framework is linear.[7] Thus, the Li always occupies the 4b position in order to maintain a linear M–C–N–Li framework; the cesium does little more than occupy space.

These geometry considerations are even more important for the Prussian Blues where the M–N interaction is roughly 4 times as great (see above). Thus, the counter transition metal in Prussian Blues will always occupy the 4b position in the *Fm3m* cell so as to maximize the M–N bond strength. As a result, for those salts where the hexacyanide to counter transition metal ratio is less than 1 (*i.e.*, $Mn_3[Co(CN)_6]_2 \cdot xH_2O$) the hexacyanide moiety will only partially occupy the 4a position. When ferrous ion is brought into contact with ferricyanide, we anticipate that $Fe^{II}_3[Fe^{III}(CN)_6]_2 \cdot xH_2O$ is formed initially, if the precipitation is much faster than electron transfer. Subsequent electron transfer would result in the conversion of $Fe^{II}_3[Fe^{III}(CN)_6]_2 \cdot xH_2O$ to the more stable ferriferrocyanide, $Fe^{II}Fe^{III}_2[Fe^{II}(CN)_6]_2 \cdot xH_2O$, and not Prussian Blue, $Fe^{III}_4[Fe^{II}(CN)_6]_3 \cdot xH_2O$. Using the above reasoning we predict a subtle, but discernible, difference between Prussian and Turnbull's Blues. In $Fe^{II}Fe^{III}_2[Fe^{II}(CN)_6]_2 \cdot xH_2O$, the 4b position will be occupied by $^1/_3$ Fe^{II} and $^2/_3$ Fe^{III} while in Prussian Blue this site is fully occupied by Fe^{III}. In both cases the 4a position is partially occupied by $[Fe(CN)_6]^{4-}$ ions; however, the multiplicity factors will be different.

As both salts are *Fm3m* and nearly identical structurally, it would be virtually impossible to distinguish the two using x-ray diffraction. However, there should be a discernible difference in Fe:C and Fe:N ratios. Unfortunately, there are several problems inherent in distinguishing Prussian and Turnbull's Blues from analysis alone. If electron transfer occurs rapidly, the conversion of Fe^{III}–C–N–Fe^{II} to Fe^{II}–C–N–Fe^{III} may compete with precipitation leading to stoichiometries between those of $Fe^{II}Fe^{III}_2[Fe^{II}(CN)_6]_2 \cdot xH_2O$ and $Fe^{III}_4[Fe^{II}(CN)_6]_3 \cdot xH_2O$. Equally important, carbon and nitrogen analyses in the presence of iron are notoriously bad. Therefore, the subtle difference between Prussian and Turnbull's Blues, from the standpoint of analysis, may have been passed over.

The most compelling evidence for the claimed similarity of Prussian and Turnbull's Blues comes from Mössbauer studies.[28-31] The question which arises now is whether or not Mössbauer studies could distinguish ferrous ion in the presence of ferri ions and ferrocyanides. The answer is not clear-cut inasmuch as the ferrous ion is in a strong field of isocyanides (see above). Furthermore, the method of preparation of the Turnbull's Blue form may obscure the answer if redox is competing with precipitation (see above) or if absorbed ions collect on the surface of the precipitate.

It is interesting to speculate on the unusual properties of a Prussian Blue type complex where the original and final states of the internal redox reaction $[M^{n+}$–C–N–$M^{m+} \leftrightarrow M^{(n-1)+}$–C–N–$M^{(m+1)+}]$ are nearly equivalent in stability. For such a system one might predict that interconversion could be effected by subtle changes, such as substitution of a different small molecule for water. This may explain the anomalous reversible color change observed for cupric ferrocyanide when exposed to ethanol; in air $Cu_2[Fe(CN)_6] \cdot xH_2O$ is brown while in EtOH it turns blue. The color change may result from partial conversion of (Cu^{II}–N–C–Fe^{II}) to (Cu^{I}–N–C–Fe^{III}) induced by the substitution of EtOH for H_2O. Certainly, the results reported here for the substitution of NH_3 for H_2O in $Cd_3[Co(CN)_6]_2 \cdot xH_2O$ show that the nature of the guest ligand may perturb the Prussian Blue lattice dramatically.

Registry No. $Cd_3[Co(CN)_6]_2$, 25359-19-7; $Mn_3[Co(CN)_6]_2$, 25868-32-0.

References and Notes

(1) A. Ludi, H. Güdel, and M. Ruegg, *Inorg. Chem.*, **9**, 2224 (1970).
(2) M. Ruegg, A. Ludi, and K. Rieder, *Inorg. Chem.*, **10**, 1773 (1971).
(3) See for example W. P. Griffith and G. T. Turner, *J. Chem. Soc. A*, 858 (1970).
(4) (a) L. H. Jones, M. M. Memering, and B. I. Swanson, *J. Chem. Phys.*, **54**, 4666 (1971); (b) L. H. Jones, B. I. Swanson, and G. J. Kubas, *ibid.*, **61**, 4650 (1974).
(5) J. J. Alexander and H. B. Gray, *J. Am. Chem. Soc.*, **90**, 4260 (1968); H. B. Gray and N. A. Beach, *ibid.*, **85**, 2922 (1963).
(6) R. L. DeKock, A. C. Sarapu, and R. F. Fenske, *Inorg. Chem.*, **10**, 38 (1971).
(7) B. I. Swanson and L. H. Jones, *J. Chem. Phys.*, **55**, 4174 (1971); **53**, 3761 (1970).
(8) B. I. Swanson and L. H. Jones, *Inorg. Chem.*, **13**, 313 (1974).
(9) B. I. Swanson and R. R. Ryan, *Inorg. Chem.*, **12**, 283 (1973); **13**, 1681 (1974).
(10) B. I. Swanson, S. I. Hamburg, and R. R. Ryan, *Inorg. Chem.*, **13**, 1685 (1974).
(11) $Cs_2M^{II}Fe(CN)_6$ (M = Zn, Cd, Mn, Co, Ni, Pd): U. G. Kuznetsov, Z. V. Popova, and G. B. Seifer, *Zh. Neorg. Khim.*, **15**, 2105 (1970).
(12) $M^{II}Pt(CN)_6$ (M = Mn, Fe, Co, Ni, Zn): H. Siebert and M. Weise, *Z. Naturforsch., B*, **27**, 865 (1972); H. Siebert and M. Weise, *ibid.*, in press.
(13) The crystals were grown by slow diffusion of $Co(CN)_6^{3-}$ and M^{II} (M = Mn, Cd) in aqueous solution. A full description will appear later.

(14) G. Beall and W. O. Milligan, unpublished results.
(15) $M^{II}_3[Co(CN)_6]_2 \cdot xH_2O$ and $Cs_2LiCo(CN)_6$ all crystallize in the space group $Fm3m$ with the $Co(CN)_6^{3-}$ moiety occupying the 4a site. In the Prussian Blues the M^{II} ion occupies the other O_h site, 4b, while Li^+ occupies this site in $Cs_2LiCo(CN)_6$. In $Cs_2LiCo(CN)_6$ the Cs^+ ions occupy the tetrahedral holes while in the Prussian Blues water occupies this site.
(16) B. I. Swanson, *Appl. Spectrosc.*, **27**, 382 (1973).
(17) B. I. Swanson, *Appl. Spectrosc.*, **27**, 235 (1973).
(18) Dehydration was also followed using x-ray crystallography. The crystals were placed in Lindemann capillaries and heated to 70°C while evacuating the capillary. No further change was observed in the lattice constant after dehydrating for 24 hr; the overall change was significant (ca. 0.2 Å): G. Beall, W. O. Milligan, and B. I. Swanson, unpublished results.
(19) For scan $(101)[(101)(10\bar{1})^s](010)$ the intensity for E_g modes is predicted to be 2.5 times as great as for scan $(10\bar{1})[(101)(101)^s](010)$; see ref 16.
(20) B. I. Swanson and J. R. Rafalko, *Inorg. Chem.*, preceding article in this issue.
(21) L. Sacconi, A. Sabatini, and P. Gans, *Inorg. Chem.* **3**, 1772 (1964).
(22) G. Ron, A. Ludi, and P. Engel, *Chimia*, **27**, 77 (1973).
(23) J. H. Schachtschneider, "Vibrational Analysis of Polyatomic Molecules. III," Technical Report No. 263-62, Shell Development Co., Emeryville, Calif., 1962.
(24) One obvious problem in comparing $F^{\nu}_{MN,MN}$ of $Cs_2MgFe(CN)_6$ and $Mn_3[Co(CN)_6]_2 \cdot xH_2O$ is the different oxidation states of the iron and cobalt atoms. Clearly, it would be more valid to compare Mn–N and Mg–N interactions where the TM hexacyanides were in the same oxidation state. However, the Mg–$[NCM'(CN)_5]$ interaction would be weaker if M' were trivalent than if M' were divalent in view of the overall charge on the $M'(CN)_6^{n-}$ moiety, and the disparity between $F^{\nu}_{MnN,MnN}$ and $F^{\nu}_{MgN,MgN}$ would be even greater. Thus, the comparison made here is on the conservative side.
(25) The close agreement between the change calculated for f_{CN} in the A_{1g} and E_g blocks (0.46 and 0.30 mdyn/Å, respectively) is reassuring (for the isolated ion $F^{A_{1g}}_{CN,CN} = f_{CN} + 4f^{cis}_{CN,C'N'} - f^{trans}_{CN,C'N'}$ and $F^{E_g}_{CN,CN} = f_{CN} - 2f^{cis}_{CN,C'N'} - f^{trans}_{CN,C'N'}$). This merely implies that a change in $F^{\nu}_{CN,CN}$ results primarily from a change in f_{CN}.
(26) W. O. Milligan, private communication.
(27) The $Cs_2LiM(CN)_6$ salts are always observed to be less soluble than the $K_3M(CN)_6$ salts.
(28) K. Maer, Jr., M. L. Beasley, R. L. Collins, and W. O. Milligan, *J. Am. Chem. Soc.*, **90**, 3201 (1968).
(29) A. Ito, M. Suenaga, and K. Ono, *J. Chem. Phys.*, **48**, 3597 (1968).
(30) J. F. Duncan and P. W. R. Wigley, *J. Chem. Soc.*, 1120 (1963).
(31) L. M. Epstein, *J. Chem. Phys.*, **36**, 2731 (1962).

Contribution from the William A. Noyes Laboratory and the Department of Physics, University of Illinois, Urbana, Illinois 61801, and from the Ralph G. Wright Laboratory, Rutgers University, New Brunswick, New Jersey 08903

Iodine-129 and Tin-119 Mössbauer Studies of Methyltin Iodides. Tin–Ligand Bond Character and the Failure of the Point-Charge Model

ALLEN P. MARKS,*[1a] RUSSELL S. DRAGO,[1b] ROLFE H. HERBER,[1c] and MARY J. POTASEK[1d]

Received May 19, 1975 AIC503475

The results of a ^{119}Sn Mössbauer study of $(CH_3)_3SnI$, CH_3SnI_3, $(C_6H_5)_3SnCl$, and $C_6H_5SnCl_3$ are reported for the neat compounds as well as for frozen solutions of these compounds in an inert solvent at liquid nitrogen temperature. The ^{129}I Mössbauer spectra of frozen solutions of the above two iodides in an inert solvent at liquid helium temperature are also reported. Molecular weight measurements indicate that the two iodides are monomers in solution. The combined study, in which NMR coupling constants along with the Mössbauer spectra of two different atoms bonded to each other in the same molecule are investigated, offers much more information than obtained from the study of only one atom in a molecule and allows checks of consistency in interpretation not offered by investigations of a single atom. The ^{119}Sn and ^{129}I Mössbauer parameters are both used to test proposed interpretations of earlier results from ^{119}Sn Mössbauer data alone which, in order to account for a p- or d-orbital imbalance, have led to much speculation about the bonding in these compounds. Furthermore, the results are used to show how and why the simple point-charge model is inadequate for interpretation of the quadrupole splitting in the ^{119}Sn Mössbauer spectra of these compounds.

Introduction

In recent years, several different models have been proposed to account for the origin of the quadrupole hyperfine interaction in ^{119}Sn Mössbauer spectra. Some of these models invoke only a p-orbital population imbalance,[2-4] whereas in other descriptions of the bonding, a d-orbital population imbalance—arising from a p_π–d_π bonding interaction—is cited[5-7] as being a major contributing factor to the magnitude of the observed quadrupole splitting.

In order to examine in greater detail which of these models (if any) do, in fact, lead to a self-consistent description of the bonding in organotin compounds, a detailed study of methyltin(IV) triiodide and trimethyltin(IV) iodide, as well as some related molecules, was undertaken. These compounds were chosen for several reasons: (a) they are symmetry related in terms of a point-charge model calculation since they both have C_{3v} symmetry with the symmetry axis coincident with the metal atom–unique ligand bond axis; (b) the ^{119}Sn quadrupole splitting is well resolved in both compounds; (c) it is possible to study the nature of the metal–ligand bonding interaction by both ^{119}Sn and ^{129}I Mössbauer effect spectroscopy, and thus the data extracted from one spectroscopic study can be used to interpret the data extracted from the other, and vice versa, thus leading ultimately to a self-consistent description; and (d) these compounds have chemical properties (e.g., stability, solubility in inert solvents, relative ease of preparation and purification, etc.) which make them suitable for such an investigation.

In addition to the Mössbauer data, it is also possible to gain some insight into the nature of the metal–ligand interactions via the tin–proton ($J_{^{117}Sn-H}$ and $J_{^{119}Sn-H}$) coupling constant extracted from nuclear magnetic resonance data, and such information can be used to estimate the electron density at the metal atom.[8] The methyltin iodides have proton NMR resonances which consist of a sharp singlet peak with symmetrical tin–proton coupling peaks on either side.

The third possible methyltin(IV) iodide, $(CH_3)_2SnI_2$, was not included in the present study since the absence of a threefold symmetry axis in this compound makes the interpretation of the ^{119}Sn Mössbauer spectra considerably more complex, especially in the absence of detailed crystallographic data related to bond angles and bond distances in this molecule.

Experimental Section

The ^{119}Sn Mössbauer spectra were obtained using a constant-acceleration spectrometer described earlier.[9] Spectrometer calibration was determined using the four inner lines of the magnetically split ^{57}Fe Mössbauer resonance in 0.8-mil NBS SRM standard iron foil at room temperature.[10] All ^{119}Sn isomer shifts are reported with respect to the center of a room-temperature $BaSnO_3$ absorption spectrum using the same $Ba^{119}SnO_3$ Mössbauer source as employed for the sample spectra.

Neat solid samples [e.g., CH_3SnI_3, $(C_6H_5)_3SnCl$, etc.] were supported between aluminum foils in a copper sample holder which in turn was attached to the tail section of a standard liquid nitrogen dewar mounted vertically, and the spectra were obtained in normal transmission geometry. Neat liquids [$(CH_3)_3SnI$, $C_6H_5SnCl_3$] and solutions of the compounds in *n*-butylbenzene were transferred by